Original Article

DOI: 10.5582/irdr.2024.01004

A novel mutation in the *OTOF* gene in a Chinese family with auditory neuropathy

Lin Deng[1,2,3], Cheng Wen[1,2,3], Yiding Yu[1,2,3], Yue Li[1,2,3], Hui Liu[1,2,3], Xinxing Fu[1,2,3], Xiaohua Cheng[1,2,3], Lihui Huang[1,2,3,*]

[1] Department of Otorhinolaryngology Head and Neck Surgery, Beijing Tongren Hospital, Capital Medical University, Beijing, China;
[2] Beijing Institute of Otolaryngology, Beijing, China;
[3] Key Laboratory of Otolaryngology Head and Neck Surgery (Capital Medical University), Ministry of Education, Beijing, China.

SUMMARY Gene therapy for monogenic auditory neuropathy (AN) has successfully improved hearing function in target gene-deficient mice. Accurate genetic diagnosis can not only clarify the etiology but also accurately locate the lesion site, providing a basis for gene therapy and guiding patient intervention and management strategies. In this study, we collected data from a family with a pair of sisters with prelingual deafness. According to their auditory tests, subject II-1 was diagnosed with profound sensorineural hearing loss (SNHL), II-2 was diagnosed with AN, I-1 was diagnosed with high-frequency SNHL, and I-2 had normal hearing. Using whole-exome sequencing (WES), one nonsense mutation, c.4030C>T (p.R1344X), and one missense mutation, c.5000C>A (p.A1667D), in the *OTOF* (NM_001287489.1) gene were identified in the two siblings. Their parents were heterozygous carriers of c.5000C>A (father) and c.4030C>T (mother). We hypothesized that c.5000C>A is a novel pathogenic mutation. Thus, subject II-1 should also be diagnosed with AN caused by *OTOF* mutations. These findings not only expand the *OTOF* gene mutation spectrum for AN but also indicate that WES is an effective approach for accurately diagnosing AN.

Keywords auditory neuropathy, *OTOF* gene, whole-exome sequencing

1. Introduction

Auditory neuropathy (AN) is a unique auditory disease in which patients can hear sounds but cannot comprehend them. AN involves both environmental and genetic factors, with more than 40% of cases caused by genetic factors (*1*). More than 20 genes have been reported to be related to AN (*2-4*). The lesion sites of AN include inner hair cells (IHCs), ribbon synapses, spiral ganglion neurons (SGNs) and demyelinated nerve axons. With the influence of time and the environment, the cells adjacent to the initial lesion site, including the outer hair cells (OHCs), will also deteriorate (*5,6*). Different pathogenic genes play a role in different parts of the auditory conduction pathway, and accurate molecular typing of AN can be performed through the analysis of pathogenic genes (*2,7-9*). The *OTOF* gene is the most common pathogenic gene for AN in different countries, and the mutation rate is as high as 41.2% in China (*10*). The main feature of AN caused by *OTOF* gene mutations is ribbon synapse lesions of IHCs, so this condition is also called auditory synaptopathy (*5,11*). Ribbon synapses are located between IHCs and primary afferent SGNs and participate in the transmission and coding of acoustic signals through exocytosis (*12*).

As a better understanding of the mechanism of AN is obtained, accurate diagnosis, intervention and effective treatment and rehabilitation have become topics of interest in the field of otology (*13-15*). The cost of developing gene therapy is extremely high, and its success depends on the accurate diagnosis of the disease by one or more specialized diagnostic tests. To date, gene therapy for monogenic AN has successfully improved hearing function in mice deficient in various target genes, such as *VGlut3*, *Otof*, and *Pjvk* (*13-15*). Appropriate candidates for gene therapy are determined by diagnostic tests, after which patients with specific defects can be treated. Thus, accurate genetic diagnosis can locate lesion sites and clarify the etiology to provide a basis for gene therapy and better guide patient intervention and management strategies (*1,16-18*).

In this study, we identified a family that potentially exhibited autosomal recessive hereditary hearing loss (HL). All the descendants in this family suffer from profound HL. To further explore the pathogenic genes of the affected individuals, we used whole-exome

sequencing (WES) to obtain mutation sites, which were subsequently screened and verified.

2. Materials and Methods

Written informed consent was obtained from the parents. The protocol was in accordance with the principles of the Declaration of Helsinki and was approved by the Ethics Committee of Beijing Tongren Hospital, Capital Medical University (Approval number: TREC2022-KY008).

2.1. Subjects

Data from a family of two sisters with prelingual deafness was collected from the Department of Otolaryngology, Head and Neck Surgery, Beijing Tongren Hospital (Beijing, China). The proband (II-2) was a 1 year old and passed the newborn hearing screening for otoacoustic emission (OAE) at birth. When she was six months old, her parents noticed that her hearing was poor, and her 12-year-old sister (II-1) exhibited similar symptoms. Patient II-1 had been wearing bilateral hearing aids for more than 10 years, but the effect was not satisfactory, as she could not speak clearly or hear easily. The father (I-1) of the participants was exposed to noise for a long time because of work, and the mother (I-2) reported normal hearing (Figure 1A).

2.2. Auditory tests and magnetic resonance imaging of the inner ear

The auditory tests included auditory brainstem response (ABR), distortion product otoacoustic emission (DPOAE), auditory steady-state response (ASSR), acoustic immittance, behavioral hearing and pure tone audiometry (PTA) tests. Acoustic immittance (226 Hz) was classified as A (including As and Ad), B, or C, where A was considered normal. The amount of 10% chloral hydrate solution used was determined according to the weight of subject II-2, and the ABR, ASSR and cochlear microphonic (CM) tests were performed while the patients slept. When the maximum sound output evoked no response, the default could not be determined. The hearing threshold was calculated as the average hearing level of PTA at 0.5, 1.0, 2.0, and 4.0 kHz according to the World Health Organization standard (2021) (*19*).

Magnetic resonance imaging (MRI) scans were obtained on a 1.5T GESigna scanner with matched eight-channel phased array coils. The protocol was designed to obtain routine axial and coronal unenhanced T2-weighted images and axial T1-weighted images, as well as axial three-dimensional fast imaging employing steady-state acquisition images of temporal bones. The cochlear nerve was also evaluated *via* MRI.

2.3. Whole-exome sequencing and variant analysis

Genomic DNA was extracted from the whole blood of four subjects and subjected to exome capture using an Agilent liquid capture system (Agilent SureSelect Human All Exon V6) according to the manufacturer's protocol. The DNA libraries were subsequently sequenced on an Illumina HiSeq sequencing platform to obtain paired-end 150 bp reads. The average sequencing depth of the target region was 127.00×, and the average coverage was 99.33%. Valid sequencing data were mapped to the reference genome (GRCh37/hg19) by BurrowsWheeler Aligner (BWA) software (*20*) to obtain the original mapping results in Binary Alignment/Map format. SAMtools (*21*) mpileup and BCFtools were used to perform variant calling and identify single-nucleotide polymorphisms (SNPs) and insertions/deletions (InDels). CoNIFER (*22*) was used to detect copy number variants (CNVs). ANNOVAR (*23*) was used to annotate SNPs, InDels and CNVs. The variant position, variant type, conservative prediction and other information

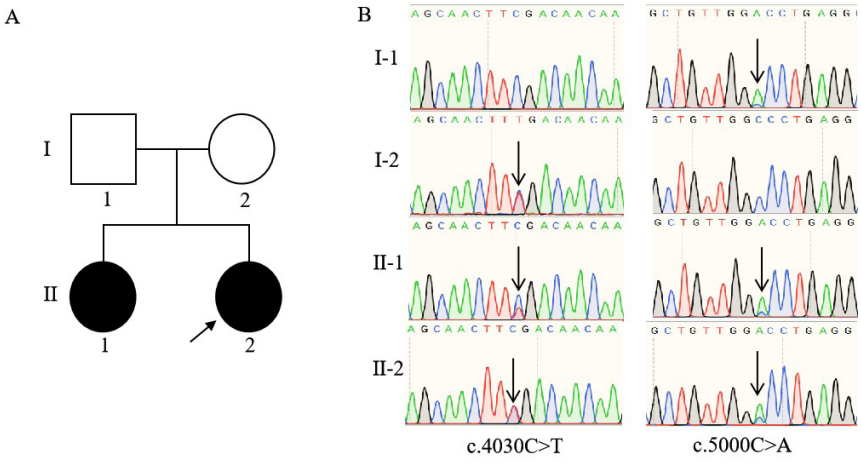

Figure 1. Pedigree and sequence analysis of *OTOF* mutations in the family. (A) Pedigree map of this family. **(B)** In this family, the compound heterozygous mutations c.4030C>T and c.5000C>A were observed in both affected siblings (II-1 and II-2); the c.5000C>A mutation was inherited from the father (I-1), and the c.4030C>T mutation was inherited from the mother (I-2).

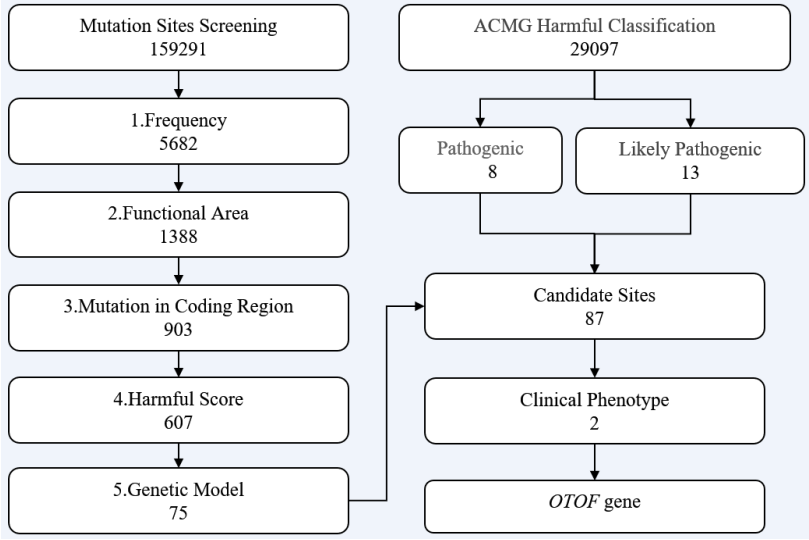

Figure 2. Variant screening process. 1. At least one mutation with a frequency higher than 1% was selected from four frequency databases: 1000g_all, ESP6500, gnomAD_ALL and gnomAD_EAS. 2. Variations in the coding region or splicing region (upper and lower 10 bp) were retained. 3. Synonymous SNP mutations not located in highly conserved regions that were not predicted by software to affect splicing and frameless InDel mutations of small fragments (< 10 bp) in the repeat region were removed. 4. Mutations were retained if they met one of the following conditions: a) predicted to be harmful or b) predicted to affect splicing. 5. Dominant inheritance: the sites with heterozygous mutations (mutation sites in sex chromosomes) in the patient's autosome and no mutations in healthy people in the family were selected as candidate sites; recessive inheritance: genes with at least two heterozygous mutation sites in patients were selected; the distribution of mutation sites on this gene in patients cannot be the same as that observed in any healthy person or a subset of the mutation sites in any healthy person. 6. Pathogenic and likely pathogenic mutations according to the ACMG guidelines were selected. 7. Steps 5 and 6 were combined to obtain candidate mutations. 8. The mutations that cosegregated with the phenotype in the pedigree were analyzed.

were obtained through a variety of databases, such as dbSNP (version 154), 1000 Genomes, GnomAD v2.1.1, CADD and HGMD. According to the American College of Medical Genetics and Genomics (ACMG) guidelines for sequence interpretation established in 2015 with the Human Genome Variation Society (HGVS) nomenclature, the mutations were categorized as pathogenic, likely pathogenic, uncertain significance, likely benign or benign. We used the existing database, software and ACMG guidelines combined with the subjects' clinical information to obtain candidate causative mutations (Figure 2). T-coffee (*24*) was used to analyze the conservation of the novel causative mutation in different species.

2.4. Sanger sequencing

The potential causative variants in this family were confirmed by Sanger sequencing of the amplified PCR products. We chose paired-end sequencing of the upstream and downstream regions of the mutation sites. The sequences of the primers used for the mutation sites in the *OTOF* gene are shown in Table 1. Each DNA sample was diluted to 20 ng/μL and used as a PCR template for amplification with Tsingke 1.1×T3 Super PCR Mix. The amplified PCR products were subjected to agarose gel electrophoresis (2 μL sample + 6 μL bromophenol blue), and the identification gel was visualized at 300 V for 12 minutes. Sanger sequencing was carried out in accordance with the band information.

Table 1. Primer sequences

Primer name	Sequence of primer	Length
c.4030-F1	5'-ACTGGTCAGAGTAAAAGCCT-3'	734 bp
c.4030-R1	5'-ATTGCTCCTAATGCTATCCC-3'	
c.4030-F2	5'-GAACTGGTCAGAGTAAAAGCC-3'	737 bp
c.4030-R2	5'-TATTGCTCCTAATGCTATCCC-3'	
c.5000-F1	5'-GCTTCTGAGGGAGACAACCC-3'	618 bp
c.5000-R1	5'-GGCTCTCCAGTCAACTTCCC-3'	
c.5000-F2	5'-GCCCAGGAAGATCAGCTCTC-3'	764 bp
c.5000-R2	5'-CCTCCCTGACCCTTCTCTCA-3'	

SnapGene was used to verify the sequencing results.

3. Results

3.1. Imaging data and audiological assessments

According to the MRI of the inner ear (Figure 3), the proband had normal cochlear nerves in both ears. Thus, retrocochlear organic diseases such as cochlear nerve dysplasia were excluded. The average ASSR thresholds were 75 dB nHL in the right ear and 77.5 dB nHL in the left ear of the proband and 95 dB nHL in the right ear and 97.5 dB nHL in the left ear of her sister (II-1). According to the behavioral hearing test and PTA results, the proband had total hearing loss, and her sister had profound hearing loss. The air conduction and bone conduction results of the ABR showed that the proband did not elicit a reproducible wave on either side at 100 dB nHL and 50 dB nHL, respectively; both sisters had a

tympanogram result of "A". The proband was diagnosed with bilateral AN according to the results of DPOAE and CM tests (Figure 4). Patient II-1 was diagnosed with AN at 2 years of age, but DPOAE and CM were absent at 12 years of age (Figure 4). Therefore, II-1 was diagnosed with sensorineural hearing loss (SNHL). Her father suffered from high-frequency (4 kHz and 8 kHz) SNHL, which may have been caused by noise exposure, and her mother's hearing remained normal.

3.2. WES and variant analysis

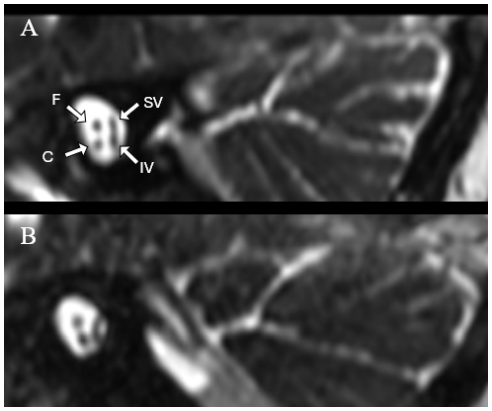

Figure 3. Oblique sagittal MRI of Patient II-2. (A) The distal slice shows the facial (F), superior vestibular (SV), inferior vestibular (IV) and cochlear (C) nerves of the right ear. **(B)** The distal slice shows the F, SV, IV, and C nerves of the left ear.

The average raw data of the sequencing samples was 11.04 Gb. The average effective data accounted for 98.93% of the data and the average Q20 was 97.85%. The average Q30 was 93.50%, and the average error rate was 0.03%. The average sequencing depth of the target region was 127.00×, and the average coverage was 99.33%. The variants were filtered as shown in Figure 2, and two mutation sites (c.4030C>T and c.5000C>A in the *OTOF* gene) were strongly related to the clinical phenotype. Both daughters presented compound heterozygosity of the nonsense mutation c.4030C>T (p.R1344X) and the missense mutation c.5000C>A (p.A1667D) in the *OTOF* gene. The c.5000C>A mutation has not been reported in HGMD, PubMed, or ClinVar; moreover, it is predicted to be harmful by SIFT, PolyPhen, and Mutation Taster and to be of uncertain significance according to the ACMG guidelines. The amino acid A1667 is conserved across multiple species (Figure 5). The pathogenicity data for the c.4030C>T mutation was collected from the databases. The patient's father was a heterozygous carrier of the c.5000C>A mutation, and the mother was a heterozygous carrier of the c.4030C>T mutation. The mutations were verified by Sanger sequencing (Figure 1B).

4. Discussion

The otoferlin protein encoded by the *OTOF* gene is an important part of the ribbon synapses, and its high

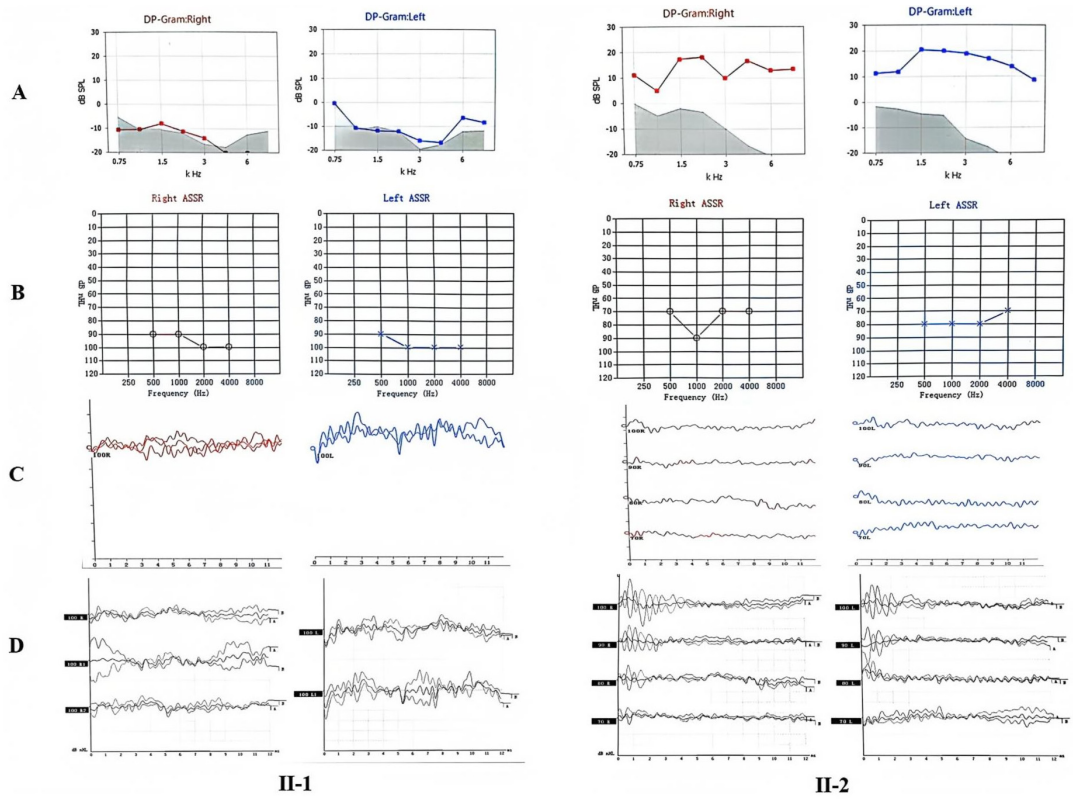

Figure 4. Audiologic tests of subjects II-1 and II-2. (A) DPOAE, distortion product otoacoustic emission; **(B)** ASSR, auditory steady-state response; **(C)** ABR, auditory brainstem response; **(D)** CM, cochlear microphonic potential.

Figure 5. Conservation analysis of the p.A1667 mutation site of otoferlin. The p.A1667 site is conserved in multiple species.

expression and proper localization are the basis for the accurate transmission of acoustic signals to auditory pathways (*25*). A mutation in the *OTOF* gene can cause structural changes and/or a decrease in otoferlin levels, weaken exocytosis of IHC ribbon synapses, and lead to different degrees of deafness (*11*). A total of 290 mutation sites in the *OTOF* gene have been reported through May 2024 (*26*), but most of them are sporadic and unique mutations.

In this study, the proband (II-2) exhibited clinical features typical of AN. Her sister (II-1) exhibited disappearance of DPOAE and CM. Severe auditory synaptopathy can eventually lead to the degeneration of IHCs and SGNs, which is why DPOAE/CM disappear in some patients during follow-up (*5*). Therefore, both of the sisters were diagnosed with AN. Two mutations in the *OTOF* gene were detected in their family by WES. The c.4030C>T mutation results in a premature stop codon by changing arginine to a terminator (p.R1344X), which leads to dysfunctional protein products that may be responsible for the pathogenesis of deafness. This mutation was previously reported in the deaf population in Pakistan and France (*27,28*), and this is the first time it has been identified in the Chinese population. The missense mutation c.5000C>A, located between the C2E and C2F domains, results in a single amino acid substitution of alanine to aspartic acid (p.A1667D) in a position that is in different species. The mutation c.5000C>A is assumed to be pathogenic because *i*) the affected individual in this family was diagnosed with AN, *ii*) the genotype and phenotype were coseparated, and *iii*) p.A1667 is conserved among different species.

Tang *et al.* developed a novel dual adeno-associated virus (AAV)-mediated gene therapy system based on the principles of protein trans-splicing that can reverse bilateral deafness in *Otof*$^{-/-}$ mice. The system effectively expressed exogenous mouse or human otoferlin and restored the release of synaptic vesicles in IHCs for a period after injection, providing a preferential clinical strategy for the treatment of *OTOF*-related AN (*15*). Since each IHC ribbon synapse is usually contacted by a single SGN, this degeneration adversely affects the effect of cochlear implantation (CI) or gene therapy (*29*). Thus, we suggested the patient (II-2) receive gene therapy at the ENT Institute and Department of Otorhinolaryngology, Eye & ENT Hospital, Fudan University, Shanghai, China. She was administered a single injection of AAV1-hOTOF into the cochlea through the round window at 3 years of age (*30*). Two months after the injection, the hearing level in both ears returned to 30 dB HL. The hearing recovery also indicates the missense mutation c.5000C>A is pathogenic.

5. Conclusion

We identified two disease-causing mutations in the *OTOF* gene in a Chinese family with AN by WES, which indicated that WES is an effective approach for identifying the hereditary characteristics of AN. The identification of these two mutations expands the known mutation spectrum of the *OTOF* gene in the Chinese population and provides a basis for gene therapy.

Acknowledgements

We are thankful for the cooperation of all members of the enrolled family. In addition, we are also so grateful to Dr. Yilai Shu (ENT Institute and Department of Otorhinolaryngology, Eye and ENT Hospital, State Key Laboratory of Medical Neurobiology and MOE Frontiers Center for Brain Science, Fudan University, Shanghai 200031, China) for his insights on our study and valuable suggestions for the manuscript revision.

Funding: This work was supported by a grant from The Natural Science Foundation of China (82071064); The Capital's Funds for Health Improvement and Research (CFH 2022-2-1092).

Conflict of Interest: The authors have no conflicts of interest to disclose.

References

1. Chinese Multi-center Research Collaborative Group on Clinical Diagnosis and Intervention of Auditory Neuropathy; Editorial Board of Chinese Journal of Otorhinolaryngology Head and Neck Surgery; Society of Otorhinolaryngology Head and Neck Surgery, Chinese Medical Association, China Division; International Association of Physicians in Audiology, Society of Audiology and Vestibular Medicine; China International Exchange and Promotive Association for Medical and Health Care. Chinese clinical practice guideline of auditory neuropathy (version 2022). Zhonghua Er Bi Yan Hou Tou Jing Wai Ke Za Zhi. 2022; 57:241-262. (in Chinese)
2. Manchaiah VK, Zhao F, Danesh AA, Duprey R. The genetic basis of auditory neuropathy spectrum disorder (ANSD). Int J Pediatr Otorhinolaryngol. 2011; 75:151-158.
3. Wang H, Bing D, Li J, Xie L, Xiong F, Lan L, Wang D, Guan J, Wang Q. High frequency of AIFM1 variants and phenotype progression of auditory neuropathy in a

Chinese population. Neural Plast. 2020; 2020:5625768.
4. Schoen CJ, Emery SB, Thorne MC, Ammana HR, Sliwerska E, Arnett J, Hortsch M, Hannan F, Burmeister M, Lesperance MM. Increased activity of Diaphanous homolog 3 (DIAPH3)/diaphanous causes hearing defects in humans with auditory neuropathy and in Drosophila. Proc Natl Acad Sci USA. 2010; 107:13396-13401.
5. Moser T, Starr A. Auditory neuropathy — neural and synaptic mechanisms. Nat Rev Neurol. 2016; 12:135-149.
6. Kitao K, Mutai H, Namba K, Morimoto N, Nakano A, Arimoto Y, Sugiuchi T, Masuda S, Okamoto Y, Morita N, Sakamoto H, Shintani T, Fukuda S, Kaga K, Matsunaga T. Deterioration in distortion product otoacoustic emissions in auditory neuropathy patients with distinct clinical and genetic backgrounds. Ear Hear. 2019; 40:184-191.
7. Starr A, Rance G. Auditory neuropathy. Handb Clin Neurol. 2015; 129:495-508.
8. Moser T, Starr A. Auditory neuropathy--neural and synaptic mechanisms. Nat Rev Neurol. 2016; 12:135-149.
9. Starr A. Auditory neuropathy and inner hair cell and synapses. Zhonghua Er Bi Yan Hou Tou Jing Wai Ke Za Zhi. 2008; 43:323-326. (in Chinese)
10. Zhang QJ, Han B, Lan L, Zong L, Shi W, Wang HY, Xie LY, Wang H, Zhao C, Zhang C, Yin ZF, Wang DY, Petit C, Guan J, Wang QJ. High frequency of OTOF mutations in Chinese infants with congenital auditory neuropathy spectrum disorder. Clin Genet. 2016; 90:238-246.
11. Vona B, Rad A, Reisinger E. The many faces of DFNB9: Relating OTOF variants to hearing impairment. Genes (Basel). 2020; 11:1411.
12. Rance G, Starr A. Pathophysiological mechanisms and functional hearing consequences of auditory neuropathy. Brain. 2015; 138:3141-3158.
13. Zhao X, Liu H, Liu H, Cai R, Wu H. Gene therapy restores auditory functions in an adult Vglut3 knockout mouse model. Human Gene Therapy. 2022; 33:729-739.
14. Delmaghani S, Defourny J, Aghaie A, *et al.* Hypervulnerability to sound exposure through impaired adaptive proliferation of peroxisomes. Cell. 2015; 163:894-906.
15. Tang H, Wang H, Wang S, Hu SW, Lv J, Xun M, Gao K, Wang F, Chen Y, Wang D, Wang W, Li H, Shu Y. Hearing of Otof-deficient mice restored by trans-splicing of N- and C-terminal otoferlin. Human Genetics. 2023; 142:289-304.
16. Huang Y, Yang J, Duan M. Auditory neuropathy: from etiology to management. Curr Opin Otolaryngol Head Neck Surg. 2022; 30:332-338.
17. Del Castillo FJ, Del Castillo I. Genetics of isolated auditory neuropathies. Front Biosci (Landmark Ed). 2012; 17:1251-1265.
18. Saidia AR, Ruel J, Bahloul A, Chaix B, Venail F, Wang J. Current advances in gene therapies of genetic auditory neuropathy spectrum disorder. J Clin Med. 2023; 12:738.
19. World Health Organization. World report on hearing. *https://iris.who.int/handle/10665/339913* (accessed October 23, 2023).
20. Li H, Durbin R. Fast and accurate short read alignment with Burrows-Wheeler transform. Bioinformatics. 2009; 25:1754-1760.
21. Li H, Handsaker B, Wysoker A, Fennell T, Ruan J, Homer N, Marth G, Abecasis G, Durbin R; 1000 Genome Project Data Processing Subgroup. The sequence alignment/map format and SAMtools. Bioinformatics. 2009; 25:2078-2079.
22. Krumm N, Sudmant PH, Ko A, O'Roak BJ, Malig M, Coe BP; NHLBI Exome Sequencing Project; Quinlan AR, Nickerson DA, Eichler EE. Copy number variation detection and genotyping from exome sequence data. Genome Res. 2012; 22:1525-1532.
23. Wang K, Li M, Hakonarson H. ANNOVAR: functional annotation of genetic variants from high-throughput sequencing data. Nucleic Acids Res. 2010; 38:e164.
24. T-coffee. *https://www.ebi.ac.uk/jdispatcher/msa/tcoffee* (accessed May 10, 2023)
25. Pangrsic T, Reisinger E, Moser T. Otoferlin: a multi-C2 domain protein essential for hearing. Trends Neurosci. 2012; 35:671-680.
26. The Human Gene Mutation Database. *https://www.hgmd.cf.ac.uk/ac/gene.php?gene=OTOF* (accessed May 14, 2024).
27. Shahin H, Walsh T, Rayyan AA, Lee MK, Higgins J, Dickel D, Lewis K, Thompson J, Baker C, Nord AS, Stray S, Gurwitz D, Avraham KB, King MC, Kanaan M. Five novel loci for inherited hearing loss mapped by SNP-based homozygosity profiles in Palestinian families. Eur J Hum Genet. 2010; 18:407-413.
28. Baux D, Vache C, Blanchet C, *et al.* Combined genetic approaches yield a 48% diagnostic rate in a large cohort of French hearing-impaired patients. Sci Rep. 2017; 7:16783.
29. Stalmann U, Franke AJ, Al-Moyed H, Strenzke N, Reisinger E. Otoferlin is required for proper synapse maturation and for maintenance of inner and outer hair cells in mouse models for DFNB9. Front Cell Neurosci. 2021; 15:677543.
30. Lv J, Wang H, Cheng X, *et al.* AAV1-hOTOF gene therapy for autosomal recessive deafness 9: a single-arm trial. The Lancet. 2024; S0140-6736(23)02874-X.

Received January 14, 2024; Revised May 15, 2024; Accepted May 17, 2024.

**Address correspondence to:*
Lihui Huang, Department of Otorhinolaryngology Head and Neck Surgery, Beijing Tongren Hospital, Capital Medical University, Beijing Institute of Otolaryngology, Key Laboratory of Otolaryngology Head and Neck Surgery (Capital Medical University), Ministry of Education, Beijing 100005, China.
E-mail: huangpub@126.com

Released online in J-STAGE as advance publication May 22, 2024.